



Dependence of impact strength on the fracture propagation direction in dynamic packing injection molded PP/EPDM blends

Yong Wang, Qin Zhang, Bing Na, Rongni Du, Qiang Fu*, Kaizhi Shen

State Key Laboratory of Polymer Materials Engineering, Department of Polymer Science and Materials, Sichuan University, Chengdu 610065, People's Republic of China

Received 7 January 2003; received in revised form 18 April 2003; accepted 23 April 2003

Abstract

In order to further understand the brittle–ductile (B–D) transition in PP/EPDM blends, a shear stress field achieved via dynamic packing injection molding was used to control the rubber particles as elongated and orientated in the PP matrix. The impact strength of the blends was measured in three fracture directions, namely, along the shear flow direction, perpendicular to and oblique (45°) with the flow direction. A definite B–D transition of impact strength was found at 20 wt% of EPDM content along the shear flow direction. About 10 times increase of impact strength was observed at the B–D transition. However, a B–D transition and then a decrease of impact strength brittle–ductile–brittle (B–D–B) was found as increasing of EPDM content in the impact direction perpendicular to and oblique with the flow direction. One observes a big increase of impact strength at 20–30 wt% of EPDM content (B–D transition) from 10–20 to 70–80 kJ/m², then a sharp decrease of impact strength is seen when EPDM content reaches to 30–45 wt% (D–B transition) from 70–80 to 40–50 kJ/m². Correspondingly, there exists a change of rubber particles from roughly spherical shape to highly elongated and oriented shape at D–B transition. SEM shows a very smooth fractured surface when fracture propagation is along or oblique with the shear flow direction, but a lay-by-layer fracture behavior when fracture propagation is perpendicular to the shear flow direction. Our results suggest that the impact fracture direction with respect to the orientation direction play an important role to determine the impact strength. Wu's theory holds true as long as the rubber particles are roughly spherical when viewed in the same direction with fracture propagation direction, but no longer valid when dispersed rubber particles are elongated and oriented when viewed in the direction perpendicular to or oblique with the fracture propagation direction.

© 2003 Elsevier Science Ltd. All rights reserved.

Keywords: PP/EPDM blends; Fracture propagation direction; Ductile–brittle transition

1. Introduction

One of the most important findings in polymer-toughening is so called critical matrix ligament thickness (T_c) theory, that developed by Wu after an investigation on Nylon 6/EPDM blends [1–4], and extended by Qi after an investigation on PP/EPDM blends [5,6]. For the first time, the model correlated the impact toughness with the phase morphology. It is proposed that T_c is the only parameter to determine the brittle–ductile (B–D) transition of the blends. Only when the matrix ligament thickness (T) is smaller than T_c , the shear yielding of matrix ligament exist and B–D transition of blends occurs. More than 10 times increase of impact strength was observed for PP/EPDM

blends at the B–D transition. Nevertheless, Wu's theory has a prerequisite: the rubber particles are considered as cubic or spherical and randomly distributed in the matrix. If the rubber particles are elongated, the stress field around a particle will not be homogeneous anymore. Much great stress concentration will be expected at the tip than the other directions. “Does the T_c criterion still holds true?” “Or what will happen?” Also, for a oriented polymer blend, the impact fracture direction with respect to the orientation direction play an important role to determine the impact strength.

Recently, the dynamic packing injection molding (DPIM) was used by our group to control the phase morphology and rubber particle orientation in iPP/EPDM and HDPE/EVA blends [7–9]. The relative impact strength of the blends was found to increase at low EPDM content, then a definite ductile–brittle (D–B) transition was

* Corresponding author. Fax: +86-28-85405402.

E-mail address: fuqiang1963@yahoo.com (Q. Fu).

observed when rubber content reaches a certain value at which the blends should fail in ductile mode by conventional molding. The results showed not only T_c but also the stress fields around individual particle play an important role to determine the impact strength of polymer blends. However, the samples in our previous work were dumbbell shaped and the impact strength of the blends can only be measured as fracture propagation perpendicular to the shear flow direction and not along or oblique to the shear flow direction. Since the fracture direction also play roles to determine the impact strength, further fracture experiments are needed on samples with different orientation with respect to the fracture propagation direction. To do this, a rectangle specimen dimension, as shown in Fig. 1, is needed, which allows us to get the impact strength both parallel and perpendicular to the shear flow directions. In this work, we will focus on the dependence of impact strength on fracture direction of PP/EPDM blends obtained by DPIM. The impact strength of the blends was measured in three fracture directions, namely, along the shear flow direction, perpendicular to and 45° with the flow direction. Very interestingly, not only a definite B–D transition of impact strength was found when the fracture propagation is

along shear flow direction, but also a brittle–ductile–brittle (B–D–B) transition was found when fracture propagation is perpendicular to or oblique with the flow direction.

2. Experimental

2.1. Materials

The polypropylene (PP) and rubber (EPDM) used in the experiment are commercial products, PP (2401) was purchased from the Yan Shan Petroleum Chemical, China (melt flow index is 2.5 g/10 min); and EPDM (EP35, JSR) was purchased from Japan Synthetic Rubber Co. Ltd, the polypropylene (C3) content is 43%.

2.2. Samples preparation

Melt blending of PP/EPDM was conducted using twin-screw extruder (TSSJ-25 co-rotating twin-screw extruder) set at a barrel temperature of 160–190 °C. After making granules, the blends were injected into a mold whose size is $68 \times 60 \times 4$ mm, using SZ 100 g injection molding machine set at 180 °C and 900 kg cm^{-2} . Then during the cooling, DPIM technology was applied, which relies on the application of shear stress fields to melt/solid interfaces during the packing stage by means of hydraulically actuated pistons. The maximum shear rate was $10\text{--}30 \text{ s}^{-1}$. The schematic representation of this technology is shown in Fig. 1. The detailed experiment procedures and the experimental devices are described in Ref. [10]. The main feature is that after the melt is injected into the mold, the specimen is forced to move repeatedly in a chamber by two pistons that move reversibly with the same frequency as the solidification progressively occurs from the mold wall to the molding core part. The processing parameters are listed in Table 1. We also carried out injection molding under static packing by using the same processing parameters but without shearing for comparison purpose. The specimen obtained by DPIM is called dynamic sample, and the specimen obtained by static packing injection molding is called static sample.

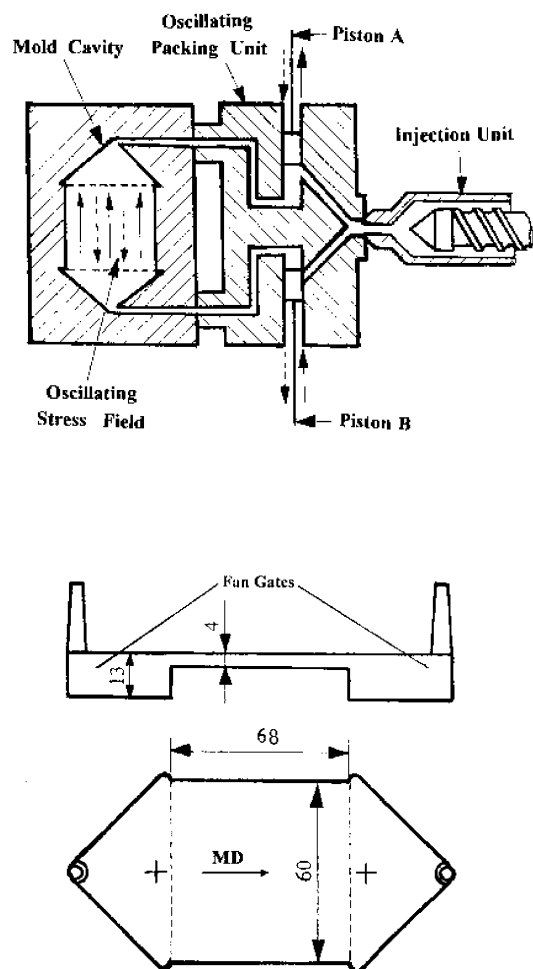


Fig. 1. The schematic representation of DPIM.

Table 1
Processing parameters in DPIM

| Processing parameters | Parameters value |
|--------------------------------|------------------|
| Injection pressure (MPa) | 90 |
| Packing pressure (MPa) | 50 |
| Melt temperature (°C) | 180 |
| Mold temperature (°C) | 20 |
| Dynamic packing pressure (MPa) | 35 |
| Dynamic packing frequency (Hz) | 0.3 |

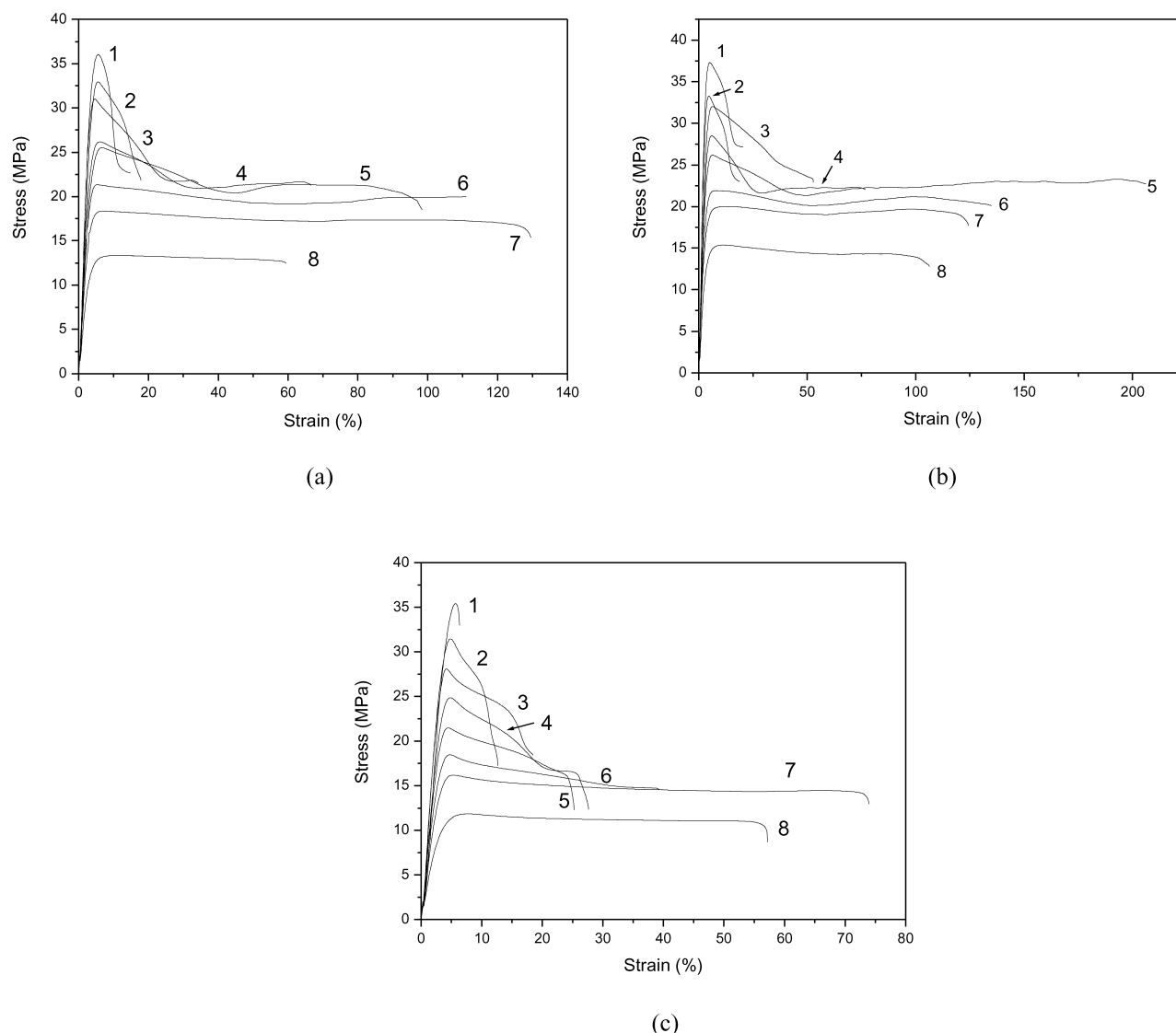


Fig. 2. The typical stress–strain curves of PP/EPDM blends, (a) static samples, (b) parallel samples and (c) vertical samples. PP/EPDM = (1) 100/0, (2) = 95/5, (3) 90/10, (4) 85/15, (5) 80/20, (6) 75/25, (7) 70/30 and (8) 60/40.

2.3. Mechanical properties measurement

Shimadzu AG-10TA Universal Testing Machine was used to measure the stress–strain curves, the moving speed was 50 mm/min and the measure temperature was 20 °C. The samples for tensile testing were rectangular with a size of 10 × 60 mm. There was necking when the stress–strain curves were measured, and the stress was plotted based on original cross-sectional area. So the engineering stress–strain curve instead of true stress–strain curve was obtained. For Izod impact strength measurement, a notch with 45° was made by machine and remained width is 8.0 mm. The experiment was carried out on an I200XJU-2.75 Impact tester according to ISO 179 and the measure temperature was 20 °C. The values of all the mechanical parameters are calculated as averages over six to nine specimens for each composition. In order to investigate the dependence of

impact strength on the heterogeneity caused by the shear flow, the samples for characterization are cut from different direction. The specimen cut along shear flow direction is called parallel sample, cut perpendicular to the shear flow is called vertical sample and cut along 45° with the flow direction is called oblique sample. Similarly, the specimens according to ASTM D638M for tensile experiment have been prepared.

2.4. SEM experiment

The phase morphologies of the blends were studied by preferential etching of the EPDM phase in toluene for two hours. The samples were fractured in the direction parallel and perpendicular to the shear direction (flow direction) in liquid nitrogen prior to etching. The impact-fractured surface was directly examined after impact experiment.

Then the morphology was observed in an SEM instrument, JSM-5900LV, operating at 20 KV.

3. Results and discussion

3.1. Typical stress–strain curves

Fig. 2 shows the typical stress–strain curves of specimens prepared by dynamic packing and static packing. For static packing, not much difference is seen for stress–strain curves between parallel samples and vertical samples due to the relative homogeneous in the samples. So stress–strain curve (and other mechanical properties, such as tensile strength and impact strength) for static samples, only in one direction (parallel to flow direction) is given in this work. The general trend is that the elongation increases as increasing of EPDM content in the composition range studied (up to 40 wt% of EPDM content), combined with the decrease of tensile stress (Fig. 2(a)). This phenomenon is quite well known and nothing special. For dynamic packing, however, a quite big difference is seen between parallel samples and vertical samples. Two things are typical for parallel samples. One is the higher tensile strength and the other is the much longer elongation compared with static samples. Further, one observes an increase of elongation at low EPDM content but decreases with the increase of EPDM content at higher EPDM content (Fig. 2(b)). A maximum of elongation is seen at EPDM content around 20–25 wt%. For vertical samples, the same stress–strain curves are observed as that for static samples (Fig. 2(c)), that is the elongation increase as increasing of EPDM content combined with the decrease of tensile stress. The tensile strengths of PP/EPDM blends along different directions obtained by DPIM are shown in Fig. 3 as a function of composition, the tensile strength of static samples is also included for comparison. One finds almost a linear decrease

of tensile strength as increasing of EPDM content for all the samples, as expected. The parallel samples have the highest tensile strength and the vertical samples have the lowest tensile strength. The oblique samples lie in-between. This can be well understood as due to the molecular chain orientation along shear flow direction. Interestingly, the vertical sample has the same tensile strength as that of static sample up to 15 wt% of EPDM content but a lower tensile strength than that of static sample when EPDM content is more than 15 wt%. The oblique sample, on the other hand, has a higher tensile strength than that of static sample up to 20 wt% of EPDM content, but a very close tensile strength as that of static sample when EPDM content is more than 20 wt%.

3.2. The impact strength

We have seen the dependence of elongation and tensile strength on the tensile direction for the dynamic samples of PP/EPDM blends, due to the molecular orientation induced by shear stress. Similarly, one expects the effect of fracture propagation direction on the impact strength. The impact strength along three fracture propagation directions is measured, that is parallel to the shear flow direction (vertical sample), perpendicular to the shear flow direction (parallel sample) and 45° with the shear flow direction (oblique sample). This is shown in Fig. 4, the impact strength for static sample is also included for comparison. A definite B–D transition of impact strength was found at 20 wt% of EPDM content measured along shear flow direction (vertical sample, Fig. 4(c)). This result is similar to the static sample (Fig. 4(d)), and in agreement with other reports obtained via conventional molding [5,6]. However, compared with the static sample, the B–D transition shifts to slightly higher EPDM content (from 10 to 15 wt%), and the impact strength is lowered down from 60 to 43 kJ/M² after the transition. Our interesting result

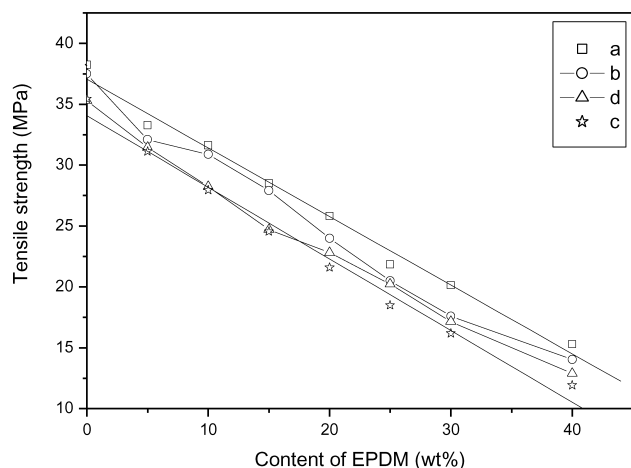


Fig. 3. The tensile strength of PP/EPDM blends as the function of EPDM content obtained by dynamic samples and static samples. (a) Parallel samples, (b) oblique samples, (c) vertical samples and (d) static samples.

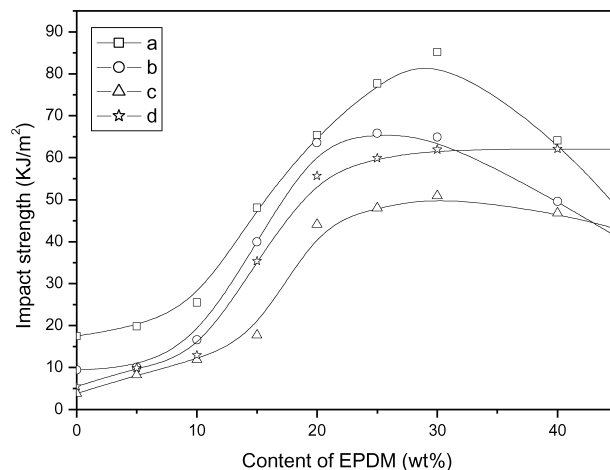
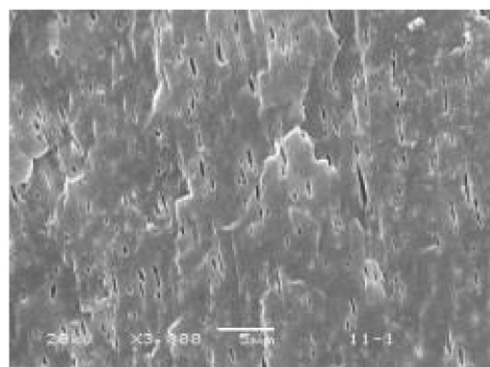
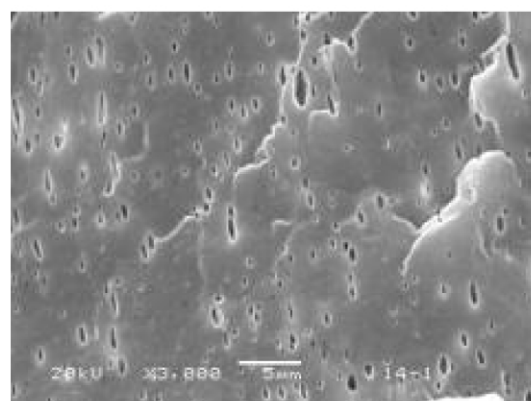


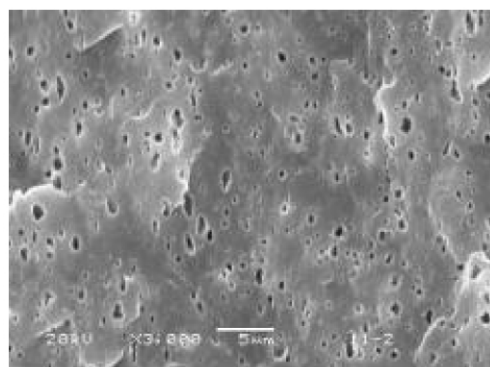
Fig. 4. The impact strength of PP/EPDM blends with different directions as a function of EPDM content. (a) Parallel samples; (b) oblique samples, (c) vertical samples, and (d) static samples.



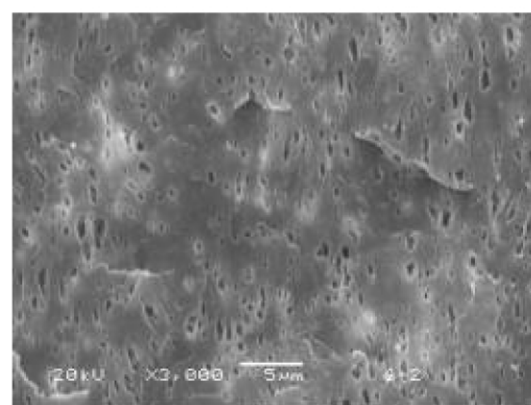
(a)



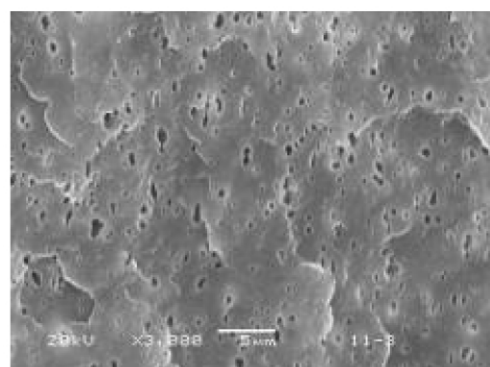
(a)



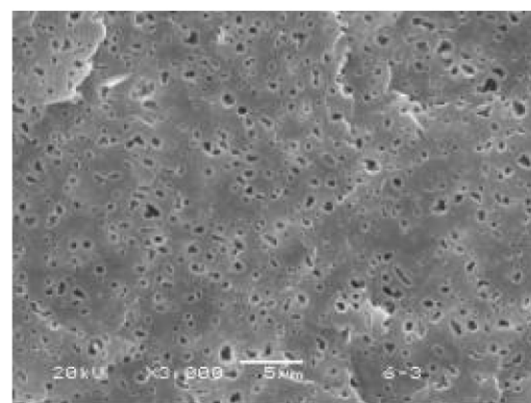
(b)



(b)



(c)



(c)

Fig. 5. SEM photographs of static sample for PP/EPDM (80/20) blends, showing three regions: (a) the skin, (b) the middle layer between the skin and the core, (c) the core.

comes when the impact strength is measured perpendicular to (parallel sample) and oblique with (oblique sample) the shear flow direction in two aspects: (1) a much higher impact strength is obtained, at the maximum, the impact strength of 80 KJ/m^2 is reached for parallel sample and 70 KJ/m^2 for oblique sample. (2) a definite B–D transition was found at 10 wt% of EPDM for both parallel sample and oblique sample, and then a D–B was seen at 30 wt% of EPDM for parallel sample and 25 wt% of EPDM for oblique sample. It should be noted that even for pure PP, the impact

Fig. 6. SEM photographs of vertical sample of PP/EPDM (80/20) blends obtained by DPIM, also showing with three regions: (a) the skin, (b) sheared layer and (c) the core.

strength for parallel and oblique samples is higher than that for vertical sample due to the molecular orientation. So, not only the EPDM rubber particles but also the orientation of PP will contribute to the impact strength. However, if one

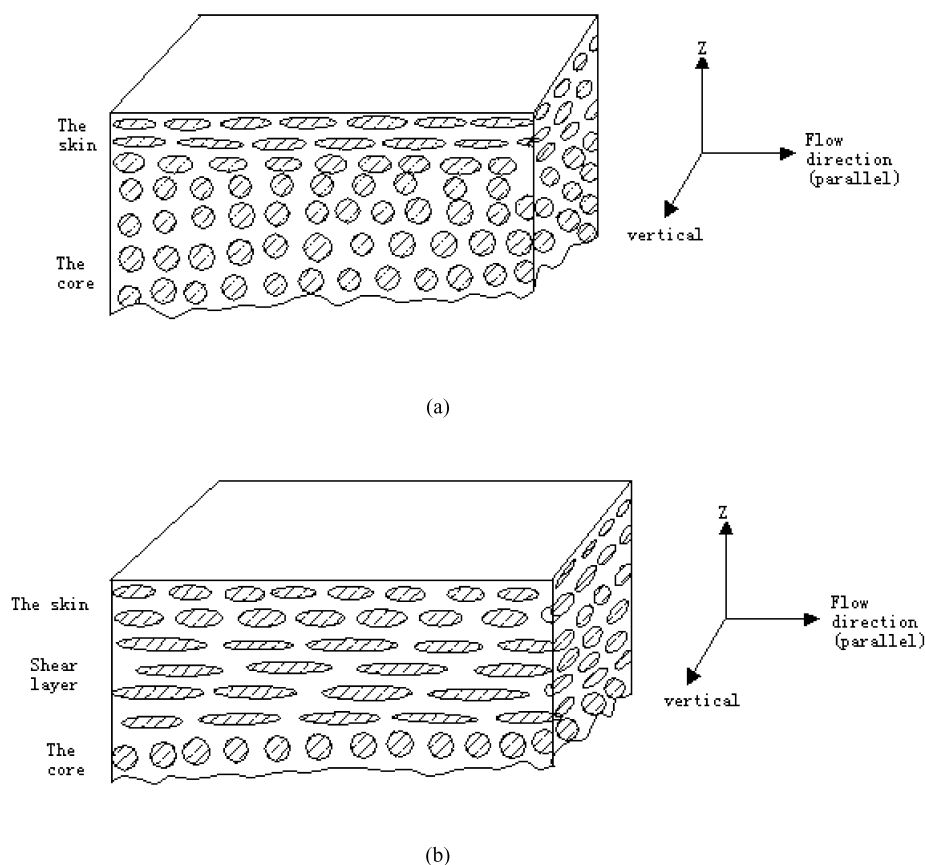


Fig. 7. The schematic representation of cross-section of PP/EPDM blends. (a) Static samples and (b) dynamic samples.

compares the relative increase of impact strength, the B–D transition or B–D–B transition is still obvious.

3.3. Phase morphology and the orientation of rubber particles

To understand the observed B–D transition in vertical samples and static samples, and B–D–B transition in parallel and oblique samples, we went to see the phase morphology of the blends. Let's take a look on the phase morphology of static sample first. The cross-section can be roughly divided into three regions, the skin, the middle layer and the core. The morphology from different regions of samples for PP/EPDM/80/20 blend is depicted in Fig. 5 and shown as an example. In the figure, the black holes represent EPDM particles, which have been dissolved out by toluene. It can be seen that in the skin, the dispersed rubber particles are highly elongated (Fig. 5(a)), due to the high shear rate from the nozzle during the injection molding. The elongated rubber particles were frozen very quickly with no time to recover back to their original shape. This result is similar to that obtained by J. Karger-Kocsis's [11]. But for the middle layer and the core, because the dispersed particles has enough time to reach equilibrium state, the deformed particles resulting from the processing will become spherical in the mold, as shown in the Fig. 5(b) and (c).

For vertical samples obtained by dynamic injection molding, one also can observe three regions in the cross-section: the skin, the sheared layer and the core. The highest shear stress is expected in the skin and lowest is in the core. The morphology from the three regions of vertical sample for PP/EPDM/80/20 blend is shown in Fig. 6 for comparison with Fig. 5. In skin, the morphology is similar to that of the static samples due to fast cooling of the surface. But in the sheared layer, the r elongated and highly oriented EPDM particles are observed. This is the result of particles orientation along the flow direction induced by shear stress during dynamic packing, and the deformed or elongated rubber particles could be fixed by the crystallization of PP during cooling, as suggested by Inoue after investigation of PP/HDPE blend [12].

In the core, because of the lowest shear stress and long time cooling, one observes less deformed and roughly spherical particles. Due to the heat released by the friction during shearing, a longer time is needed for cooling down the dynamic sample, which gives the sample more time to recover back to its original shape. The schematic representation of three-dimensional morphology of PP/EPDM, for both static and dynamic samples is shown in Fig. 7, for comparison.

So, the morphology difference between the static sample and the dynamic sample will be mainly in the region of

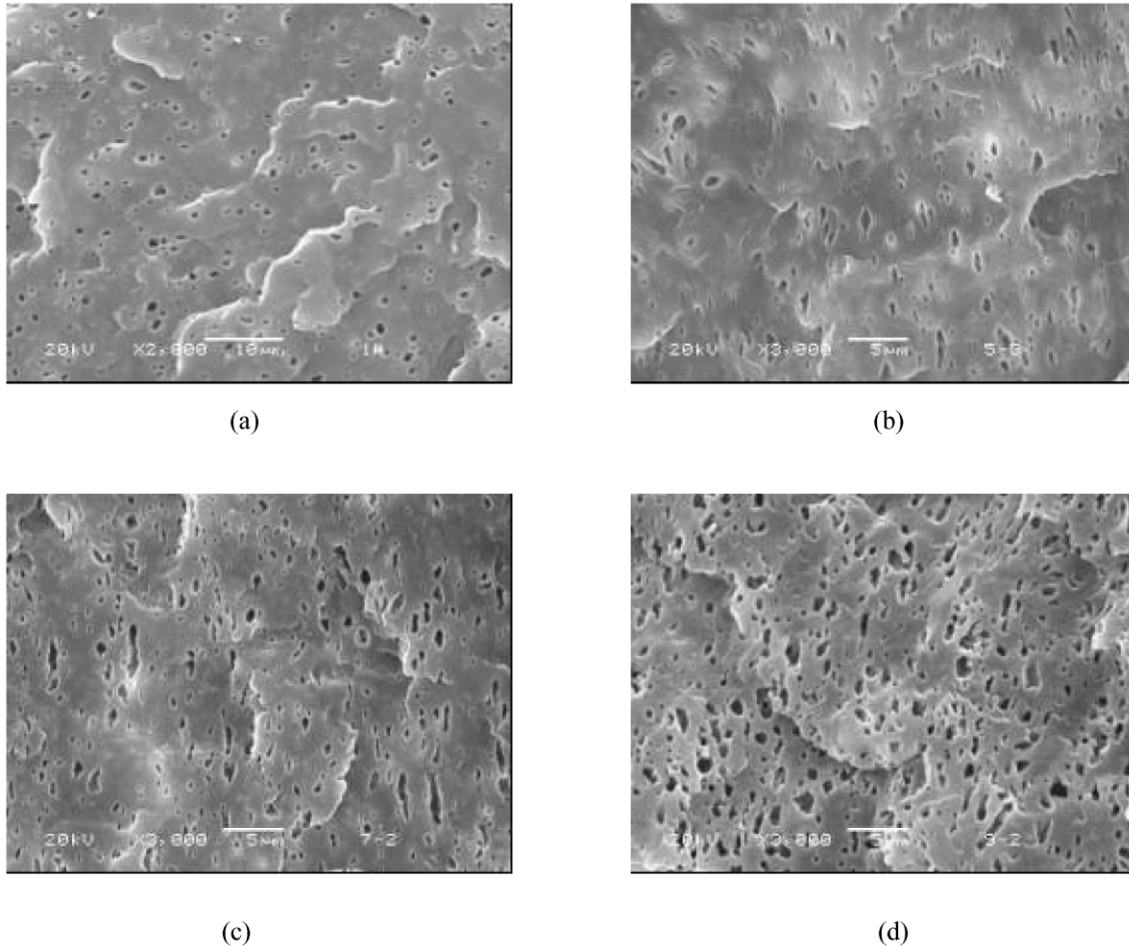


Fig. 8. SEM photographs viewed perpendicular to the shear flow direction of PP/EPDM blends obtained via DPIM. EPDM content: (a) 10%, (b) 20%, (c) 30% and (d) 40%.

sheared layer. Following, we will focus on the change of phase morphology in sheared layer as function of EPDM content. Fig. 8 shows the SEM photographs viewed perpendicular to the shear flow direction of PP/EPDM blends obtained via DPIM. Note, this direction is the same with fracture propagation direction for vertical sample. In all the compositions studied, the rubber particles are roughly spherical and the size is kept relatively constant (about $1.0\ \mu\text{m}$). This is in agreement with Borggreve's [13] and Tang's [14] results showing that the coalescence during blending of two polymer melts are prevented when there is sufficient interfacial adhesion between the dispersion and the matrix phase. Above, we see the B–D transition for vertical sample in Fig. 4, it seems that Wu's theory will hold true as long as the rubber particles are roughly spherical when viewed in the same direction with fracture propagation direction. The shift to a slight higher EPDM content at B–D transition compared with static samples is probably due to the change of matrix toughness of PP caused by the molecular orientation in the shear stress, which may result in the change of critical matrix ligament thickness (T_c).

Fig. 9 shows the SEM photographs viewed along with the shear flow direction of PP/EPDM blends obtained via

DPIM. Note this direction is perpendicular to the fracture propagation direction for parallel sample. At lower EPDM content (i.e. 10 wt%), most of rubber particles are spherical and a few particles are elliptical. The size is in the range of $0.3\text{--}1.0\ \mu\text{m}$, and not homogeneous. With the increasing EPDM content, more elongated and oriented rubber particles are observed. Especially, when the EPDM content reaches to 30 and 40 wt%, all the rubber particles are elongated and highly oriented along the shear flow direction, where one observes a D–B transition in Fig. 4. Here the result indicates once again that the Wu's criterion is no longer valid when dispersed rubber particles are elongated and oriented when viewed in the direction perpendicular to the fracture propagation direction.

3.4. The toughening mechanism

According to Wu's theory, for given blends, T_c is independent of the volume fractions and particle size of the rubber. If the neighboring particles are taken into account, the stress fields around individual particle are expected to interfere or overlap with each other and hence more massive shear yielding is expected to pervade the matrix as T is

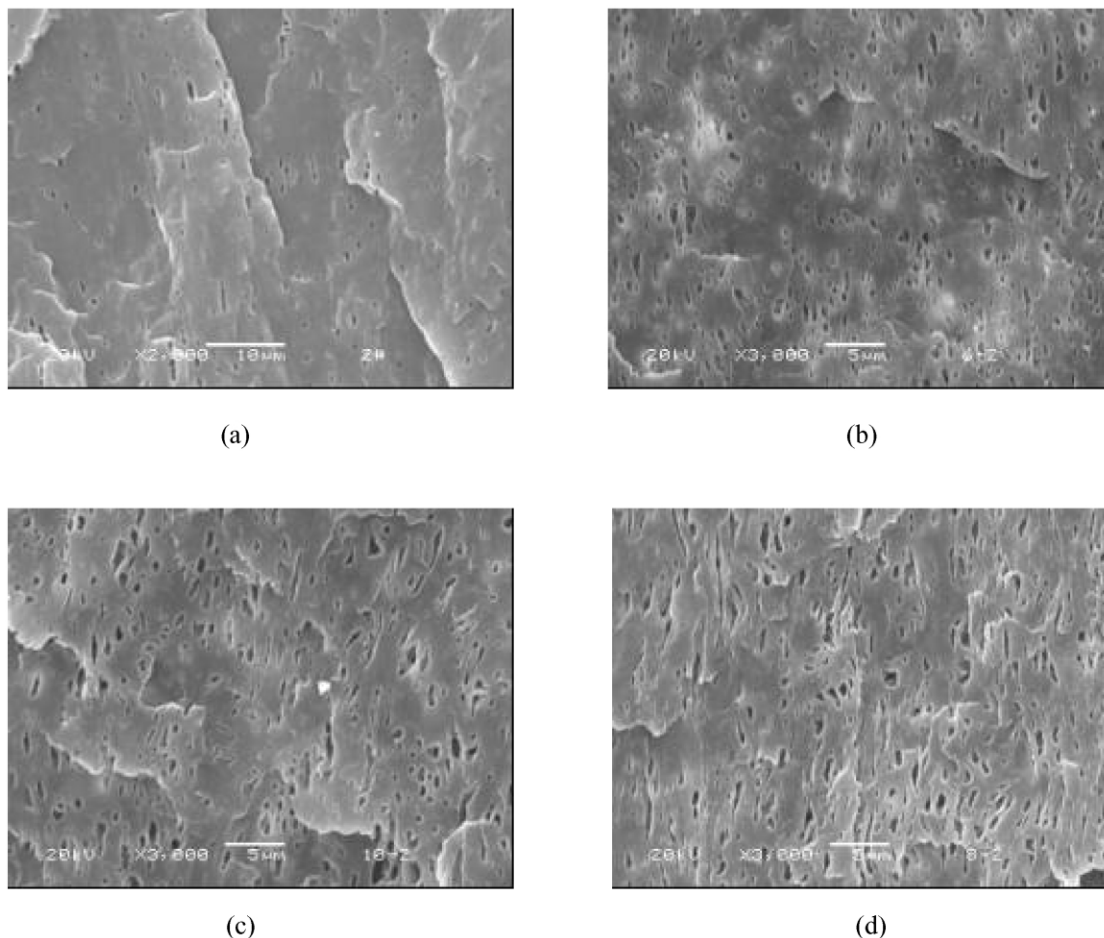


Fig. 9. SEM photographs viewed along with the shear flow direction of PP/EPDM blends obtained via DPIM. EPDM content: (a) 10%, (b) 20%, (c) 30% and (d) 40%.

decreased. A percolation process of stress volume spheres has been successfully used to explain the phenomenon of the B–D transition [15–17]. The theory, which has also created much controversy, has been further clarified by Muratoglu et al [18–20], who have proposed that the incoherent particle-matrix interfaces stimulate a preferential form of crystallization over a definite distance around the particles with the lowest energy surfaces of crystalline lamellae representing also the crystallographic planes of

lowest plastic resistance lying parallel to the interfaces. Above, we demonstrated the dependence of impact strength on the fracture propagation direction in oriented PP/EPDM blends. Wu's theory holds true as long as the rubber particles are roughly spherical when viewed in the same direction with fracture propagation direction, but no longer valid when dispersed rubber particles are elongated and oriented when viewed in the direction perpendicular to the fracture propagation direction. The relation between the

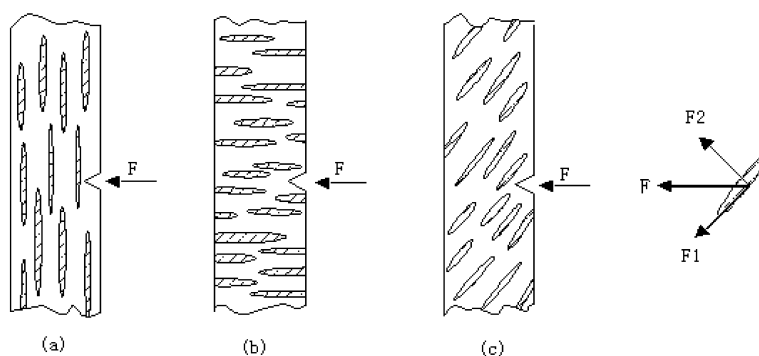


Fig. 10. The schematic representation of the relation between the rubber particle orientation and the fracture propagation direction. (a) Parallel samples, (b) vertical samples and (c) oblique samples.

rubber particle orientation and the fracture direction is schematically shown in Fig. 10. For the parallel samples, the fracture propagation direction is perpendicular to the orientation direction of rubber particles and the matrix. Much energy is expected to break down the sample in the direction perpendicular to the orientation of rubber particles and the matrix. But for the vertical samples, the fracture propagation direction is along the orientation direction of rubber particles and the matrix. Because of the weak Van der Waals force between the rubber particles and the matrix, the crack caused by impact force enlarges along the interface between the elongated rubber particles and the matrix, and results in a lower value of impact strength. For the oblique samples, the impact force can be divided into two parts. One is along the shear flow direction and the other is perpendicular to the flow direction. If we assume that only the force along the flow direction will cause sample fracture (it seems true because it is the weakest direction for a oriented sample), the fracture propagation direction will be along the flow direction and will be 45° with the impact direction. This results in higher impact strength than that of vertical samples, but lower impact strength than that of parallel samples. We have indeed observed that the fracture of oblique samples is along the flow direction instead of impact direction for both tensile experiment and impact experiment, as schematically shown in Fig. 11. Experimentally, one observes totally different fractured surfaces of samples fractured in three directions, which indicates different fracture mechanisms. Fig. 12 depicts the SEM photographs of impact-fractured surface of PP/EPDM = 85/15, shown as an example. For vertical sample, a very smooth surface with many holes is seen, which is a typical morphology for brittle fracture (Fig. 12(a)). The holes are probably due to the detachment of rubber particles during the impact fracture. For oblique sample, a smooth surface with some yielding sheets is seen (Fig. 12(b)), which

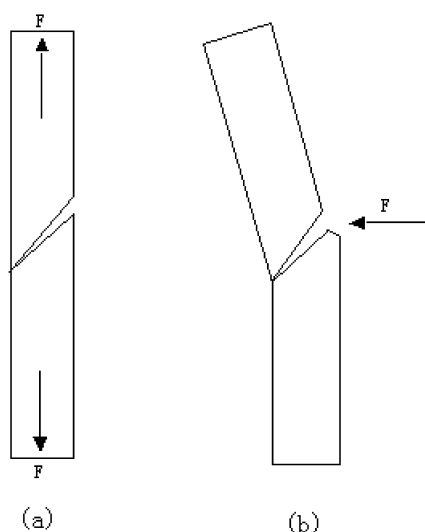
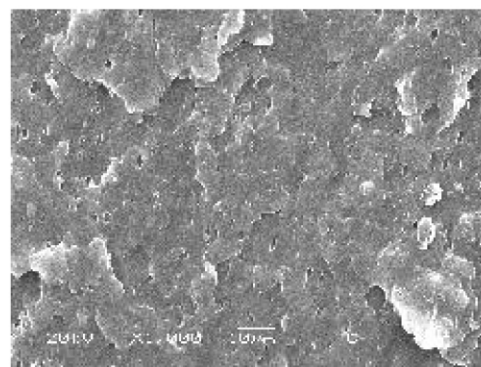
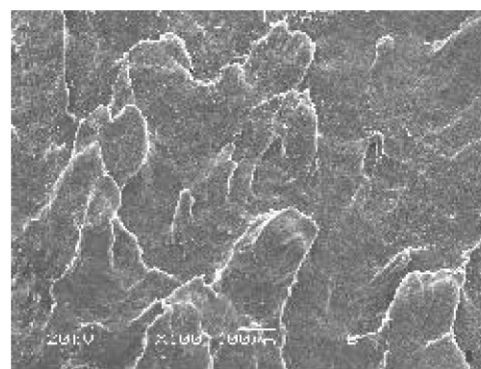


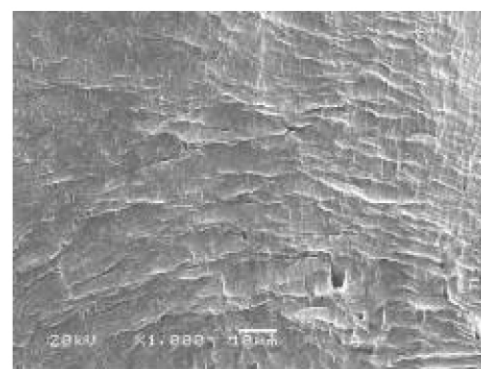
Fig. 11. The schematic representation of the fracture of oblique samples, (a) tensile experiment and (b) impact experiment.



(a)



(b)

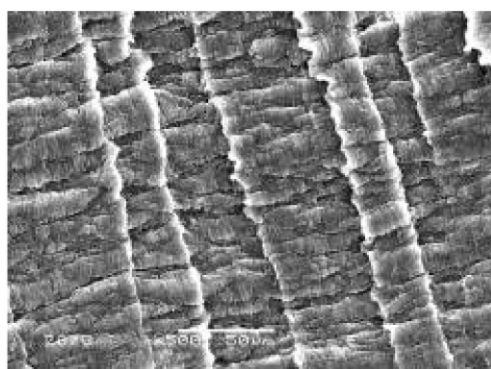


(c)

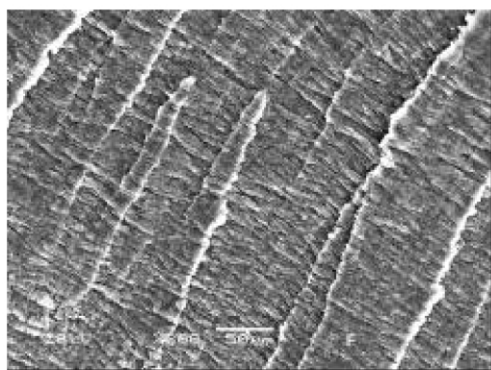
Fig. 12. SEM photographs of impact-fractured surface of PP/EPDM = 85/15, (a) vertical sample (b) oblique sample and (c) parallel sample.

still suggests a brittle behavior. For parallel sample, however, one observes many thin and long strips which are parallel to each other and are homogeneously distributed (Fig. 12(c)), which suggests that the crack may start from one elongated particle but stop as it meets another elongated particle nearby, when the fracture propagation direction is perpendicular to the shear flow. The result indicates the development of crack is a layer-by-layer process by which a lot of impact energy is dissipated.

Now the remaining question is that how can we understand the D–B transition for parallel and oblique samples. From phase morphology, one observes a big change of rubber particles from roughly spherical shape to highly elongated and oriented at D–B transition. Compared with the impact-fractured surface of the parallel samples between PP/EPDM = 85/15 with 70/30 or 60/40, the difference is obvious, as shown in Fig. 13, where the strips are connected for both samples due to the relatively high concentration of oriented and elongated rubber particles. Here all the strips are interfered or overlapped with each other and hence more massive fracture is expected to pervade the matrix, as the two strips are close enough. This may be the reason for D–B transition. The finite element method (FEM) analysis showed that during impact fracture, dispersed particles acted as a stress concentrators to cause the three-dimensional stress concentration of matrix ligament around it. The stress concentration occurs not only in the equatorial (90°) but also in the polar (0°) and 45° direction around the dispersed particle. It is concluded that the first stress and the equivalent stress become the dominating in rubber-toughened plastics, and they reach their maximum value at the equator region [21,22]. Obviously, the elongated rubber particles will cause a



(a)



(b)

Fig. 13. SEM photographs of impact-fractured surface of parallel samples for PP/EPDM blends (a) = 70/30 and (b) 60/40.

strong concentration of stress at the tip. Future work is needed to verify this expectation. Two other factor may also affect the impact strength: (1) the thickness of sheared layer, and (2) the crystal morphology of PP. For the thickness of sheared layer, we assume it is big enough to dominate the mechanical properties in our work. For the crystal morphology, it usually keeps unchanged under the same processing conditions and does not change much as increasing EPDM content.

4. Conclusion

The dependence of impact strength of PP/EPDM blends on the fracture propagation direction in oriented samples obtained via DPIM was demonstrated in this work. A definite B–D transition of impact strength was observed in vertical sample, where the fracture propagation direction is along shear flow direction; and a B–D–B transition was seen in parallel and oblique sample, where the fracture propagation direction is perpendicular to or oblique with the shear flow direction. Morphologically, one observes always roughly spherical rubber particles with constant size viewed perpendicular to the shear flow direction, and highly elongated and oriented rubber particles viewed along shear flow direction at higher EPDM content (more than 30 wt%). A very smooth fractured surface is observed when fracture propagation is along or oblique with the shear flow direction, but a lay-by-layer fracture behavior, when fracture propagation is perpendicular to the shear flow direction. It seems that Wu's theory holds true as long as the rubber particles are roughly spherical when viewed in the same direction with fracture propagation direction, but no longer valid when dispersed rubber particles are elongated and oriented when viewed in the direction perpendicular to or oblique with the fracture propagation direction.

Acknowledgements

We would like to express our great thanks to the China National Distinguished Young Investigator Fund, National Natural Science Foundation of China (No. 20274028) and special funding from Ministry of Education for Doctor-Degree (No. 20020610004 and 2000061021) for Financial Support.

References

- [1] Wu S. J Appl Polym Sci 1990;30:73.
- [2] Wu S. Polymer 1985;26:1855.
- [3] Wu S. J Appl Polym Sci 1988;35:549.
- [4] Wu S. Polymer 1990;31:972.
- [5] Wu X, Zhu X, Qi ZN. The 8th International Conference on Deformation, Yield and Fracture Behavior of Polymers, Cambridge, UK; 1991 p. 78/1.

- [6] Zheng WG, Li Q, Qi ZN. Chin Sci Bull 1992;37:904.
- [7] Fu Q, Wang Y, Li QJ, Zhang G. Macromol Mater Eng 2002;287:391.
- [8] Wang Y, Fu Q, Li QJ, Zhang G. J Polym Sci, Part B: Polym Phys 2002;40:2086.
- [9] Na B, Zhang Q, Fu Q. Polymer 2002;43:7367.
- [10] Guan Q, Shen KZ, Li J, Zhu J. J Appl Polym Sci 1995;55:1797.
- [11] Karger-Kocsis J, Csikai I. Polym Eng Sci 1987;27:241.
- [12] Sano H, Yui H, Li HG, Inoue T. Polymer 1998;39:5265.
- [13] Borggreve RJM, Gaymans RJ, Schuijjer J, Ingen Housz JF. Polymer 1987;28:1489.
- [14] Tang T, Huang BT. Polymer 1994;35:281.
- [15] Margolina A, Wu S. Polymer 1988;29:2190.
- [16] Zheng WG, Li Q, Qi ZN. J Polym Eng 1993;12:230.
- [17] Fu Q, Wang G. Polym Int 1993;30:309.
- [18] Muratoglu OK, Argon AS, Cohen RE, Weinberg M. Polymer 1995;36:921.
- [19] Muratoglu OK, Argon AS, Cohen RE. Polymer 1995;36:2143.
- [20] Muratoglu OK, Argon AS, Cohen RE, Weinberg M. Polymer 1995;36:4787.
- [21] Eshelby JD. Proc Roy Soc 1957;A241:376.
- [22] Zhang R, Lu S. Appl Com Mater 1994;1:115.